Scientific Report No. 3
Contract N140(70024)75686B
January 1966

applied • mathematics

Further Results on Acoustic Radiation from a Finite Cylinder

by

Charles H. Sherman
Dorothy A. Moran

for

U. S. Navy Underwater Sound Laboratory

3.00 0.75 57 as

code 1

PARKE MATHEMATICAL LABORATORIES, Inc.
One River Road • Carlisle, Massachusetts

PARKE MATHEMATICAL LABORATORIES, INCORPORATED
ONE RIVER ROAD • CARLISLE, MASSACHUSETTS

Requests for additional copies by Agencies of the Department of Defense, their contractors, and other Government agencies should be directed to the:

DEFENSE DOCUMENTATION CENTER (DDC)
CAMERON STATION
ALEXANDRIA, VIRGINIA 22314

Department of Defense contractors must be established for DDC services or have their 'need-to-know' certified by the cognizant military agency of their project or contract.

All other persons and organizations should apply to the:

CLEARINGHOUSE FOR FEDERAL SCIENTIFIC
AND TECHNICAL INFORMATION (CFSTI)
SILLS BUILDING
5285 PORT ROYAL ROAD
SPRINGFIELD, VIRGINIA 22151

A limited number of copies are also available by writing to:

PARKE MATHEMATICAL LABORATORIES, INC.
ONE RIVER ROAD
CARLISLE, MASSACHUSETTS 01741

Scientific Report No. 3
Contract N140(70024)75686B
January 1966

applied • mathematics

Further Results on Acoustic Radiation from a Finite Cylinder

by

Charles H. Sherman
Dorothy A. Moran

for

U. S. Navy Underwater Sound Laboratory

PARKE MATHEMATICAL LABORATORIES, Inc.
One River Road • Carlisle, Massachusetts

SCIENTIFIC REPORTS

their purpose and place

•••A•P•P•L•I•E•D••M•A•T•H•E•M•A•T•I•C•I•A•N•S•••

THE EVER INCREASING NEED TO BE INFORMED has caused an ever increasing volume of publications. The very quantity of these publications, however, makes it difficult to satisfy the need, because it becomes more and more arduous to locate the literature pertinent to any one subject; and because any one of us becomes more and more weary of having so much to read. Moreover, only a small minority of these publications may help satisfy the need, because an overwhelming majority is void of content.

Consequently, it is imperative to present to the public only manuscripts which do carry new information without undue verbiage; hoping to be judged not by the number of published pages but by their quality. In particular, papers in the field of Applied Mathematics ought to be published only if they contain one or more of the following items: new basic results, new methods, new applications, new numerical results, new presentation of difficult and important topics, up-to-date bibliographies; and if the number of their pages is not dictated by the desire of imposing upon the superficial reader.

To discharge our contractual obligations, we publish *Technical or Scientific Reports*, such as the one you now have in your hands. It has been our constant policy to see to it, that they satisfy the above strict criterion.

PARKE MATHEMATICAL LABORATORIES, INC.
bedford road, carlisle, massachusetts

Abstract

The earlier work on acoustic radiation from a cylinder was extended by working out the low frequency approximation and doing more machine calculations. A variety of boundary conditions and cylinder height to diameter ratios were treated in the low frequency approximation, and the results were used to study the limitations of the method of calculation. The machine calculations were performed for cases in which the method should yield reliable far field results. Several different cases of cylinders vibrating symmetrically on the ends with uniform and parabolic velocity distributions were treated. Directivity patterns and radiation resistances were obtained which should be useful in transducer design work.

Table of Contents

BLANK PAGE

PARKE MATHEMATICAL LABORATORIES, INCORPORATED
ONE RIVER ROAD • CARLISLE, MASSACHUSETTS

Further Results on Acoustic Radiation from a Finite Cylinder

by

Charles H. Sherman and Dorothy A. Moran

Introduction

The method for the calculation of acoustic radiation from a finite cylinder[1,2] has been extended by working out the details of the low frequency approximation as described in preliminary fashion earlier[3]. Although this approximation holds only when the height and diameter of the cylinder are both much smaller than the wavelength, it has the advantage of giving results in a partially analytical form. Such results have been obtained for cylinders with six different ratios of height to diameter (b/a = 4,2, 3/2, 1, 1/2 and 1/4) and six different boundary conditions (uniform and parabolic vibration of the cylinder sides and uniform and parabolic vibration of the cylinder ends with both symmetric and antisymmetric forms of the latter). These low frequency results provide the opportunity for evaluating the method more fully than has been possible before. We will be able to determine how the accuracy of the results depends on the type of boundary condition and on the ratio of cylinder height to diameter. Such information will be an important guide for future applications of the method.

The computer program[2] for the calculation of acoustic radiation from a finite cylinder has also been revised and used to obtain numerical results for cylinders vibrating on the ends. Several examples of far field radiation patterns and various radiation resistance results have been obtained which will be useful in transducer design work. It has not been possible to obtain accurate near field results with the revised program because of practical machine limitations. Although these limitations might be partially overcome by further revisions of the program, the studies to be described here suggest other directions which might ultimately be more fruitful.

Summary of Method

In brief summary the method consists of expanding the spatial part of the acoustic velocity potential in the finite series of spherical wave functions

$$\psi(r, \theta) = \sum_{n=0}^{N} a_n P_n(\cos\theta)\, h_n(kr), \tag{1}$$

for axially symmetric boundary conditions. In Eq.(1) r and θ are spherical coordinates with origin at the center of the cylinder and polar axis parallel to the cylinder axis, $P_n(\cos\theta)$ is the Legendre polynomial, and $h_n(kr)$ is the spherical Hankel function. The boundary conditions are satisfied in the least squares sense when the expansion coefficients, a_n, are determined from the equations

$$\sum_{n}^{N} a_n(\phi_m, \phi_n) = (\phi_m, N(\theta)), \quad m = 0, 1, 2, \ldots, N, \tag{2}$$

where

$$(\phi_m, \phi_n) = \iint \phi_m^*(\theta)\, \phi_n(\theta)\, dS, \tag{3}$$

$$(\phi_m, N(\theta)) = \iint \phi_m^*(\theta)\, N(\theta)\, dS, \tag{4}$$

$\phi_n(\theta)$ is the normal derivative of $P_n(\cos\theta) h_n(kr)$ evaluated on the boundary, $N(\theta)$ is the specified axially symmetric normal velocity on the boundary, and the integrations extend over the entire boundary surface.

The scalar products in Eqs.(3) and (4) have the properties:

1) $(\phi_n, \phi_m) = (\phi_m, \phi_n)^*$
2) $(\phi_m, \phi_n) = 0$ except when m and n are both even or both odd
3) $(\phi_m, N(\theta)) = 0$ for odd (even) m when $N(\theta)$ is symmetric (antisymmetric) with respect to the equatorial plane.

It follows from the second property that Eq.(2) separates into two sets of equations - one involving only even order coefficients, the other only odd order coefficients. The third property then shows that for a symmetric (antisymmetric) problem the odd (even) order set of equations is homogeneous, and the odd (even) order coefficients vanish. It is convenient to treat boundary conditions which are either symmetric or antisymmetric and then handle more general boundary conditions by superposition.

The general expression for $\phi_n(\theta)$ for a cylindrical boundary of height $2b$ and radius a is:[1]

$$\phi_n(\theta) = \begin{cases} k\cos\theta\, h_n'\left(\frac{kb}{\cos\theta}\right) P_n(\cos\theta) + \frac{\sin^2\theta\cos\theta}{b}\, h_n\left(\frac{kb}{\cos\theta}\right) P_n'(\cos\theta), & 0 \le \theta \le \theta_o = \tan^{-1} a/b, \\ \\ k\sin\theta\, h_n'\left(\frac{ka}{\sin\theta}\right) P_n(\cos\theta) - \frac{\sin^2\theta\cos\theta}{a}\, h_n\left(\frac{ka}{\sin\theta}\right) P_n'(\cos\theta), & \theta_o \le \theta \le \pi/2, \end{cases} \tag{5}$$

and for $\pi/2 \le \theta \le \pi$ the expression is given in terms of Eq.(5) by $(-1)^n \phi_n(\pi-\theta)$. Eq.(5) is used in the computer program. An approximation which holds for small ka and small kb will be discussed in the next section.

Low Frequency Approximation

We begin the low frequency approximation by using the standard small argument formulas for the spherical Hankel functions and their derivatives in Eq.(5). If the cylinder height and diameter are both sufficiently small compared to the wavelength, any point on the cylindrical boundary is close enough to the origin to validate this approximation. The expansion coefficients obtained by satisfying the boundary conditions in this approximation can then be used in Eq.(1) to calculate the sound field at any point outside the cylinder.

The small argument formulas for the spherical Hankel functions and their derivatives are[4]:

$$h_n(x) = -i\, D_n\, e^{i\delta_n} \tag{6}$$

$$d/dx\; h_n(x) = h_n'(x) = -i\, D_n'\, e^{i\delta_n'} \tag{7}$$

where

$$D_n = \frac{1 \cdot 1 \cdot 3 \cdot 5 \cdots (2n-1)}{\chi^{n+1}}$$

$$D'_n = \frac{n+1}{\chi} D_n$$

$$\delta_0 = \chi$$

$$\delta_n = \frac{\chi^{2n+1}}{1 \cdot 3 \cdot 5 \cdots (2n+1) \cdot 1 \cdot 1 \cdot 3 \cdot 5 \cdots (2n-1)}, \quad n > 0$$

$$\delta'_0 = 1/3\, \chi^3$$

$$\delta'_n = -\frac{n}{n+1} \delta_n, \quad n > 0.$$

These formulas hold for $\chi \ll |2n-1|$, except for $h_0(\chi)$ which is given exactly.

We will approximate the spherical Hankel functions and their derivatives further by replacing the complex exponentials in Eqs.(6) and (7) by unity which is consistent with the restriction to sufficiently small ka and kb. With this additional approximation the expressions in Eqs.(6) and (7) have the same form as the small argument approximations of the radial solutions of Laplace's equation. Our approximation is, then, the familiar one in which the acoustic field near the source is replaced by a hydrodynamic field. With these approximations Eq.(5) reduces to

$$\Phi_n(\theta) = \begin{cases} 1 \cdot 1 \cdot 3 \cdot 5 \cdots (2n-1)\, ik \left(\frac{\cos\theta}{kb}\right)^{n+2} (n+1) P_{n+1}(\cos\theta), & 0 \le \theta \le \theta_0 \\ 1 \cdot 1 \cdot 3 \cdot 5 \cdots (2n-1)\, ik \sin\theta \left(\frac{\sin\theta}{ka}\right)^{n+2} P'_{n+1}(\cos\theta), & \theta_0 \le \theta \le \pi/2 . \end{cases} \tag{8}$$

Although Eq.(8) is significantly simpler than Eq.(5) it is still not feasible to obtain the expansion coefficients in an analytical form as functions of ka and b/a. It is only feasible to specify a numerical value of b/a and then obtain the results as a function of ka. This has been done for six different values of b/a for which the cylinders are illustrated to scale in Fig 1. For each value of b/a the calculations have been performed for six different boundary conditions - the following four conditions which are symmetric with respect to the equatorial plane:

uniform vibration of sides $N(\theta) = \begin{cases} 0, & 0 \le \theta \le \theta_0 = \tan^{-1} a/b \\ u, & \theta_0 \le \theta \le \pi/2 \end{cases}$

parabolic vibration of sides $N(\theta) = \begin{cases} 0, & 0 \le \theta \le \theta_0 \\ u(1 - \cot^2\theta / \cot^2\theta_0), & \theta_0 \le \theta \le \pi/2 \end{cases}$

uniform vibration of ends $N(\theta) = \begin{cases} u, & 0 \le \theta \le \theta_0 \\ 0, & \theta_0 \le \theta \le \pi/2 \end{cases}$

parabolic vibration of ends $N(\theta) = \begin{cases} u(1 - \tan^2\theta / \tan^2\theta_0), & 0 \le \theta \le \theta_0 \\ 0, & \theta_0 \le \theta \le \pi/2 \end{cases}$

plus the antisymmetric forms of the latter two conditions. These six normal velocity distributions are illustrated in Fig 2.

In each of these 36 cases we have used from one to five terms in the expansion in Eq.(1). The results for the expansion coefficients are given in Tables 1-6 in Appendix I. In this approximation we obtain only the imaginary parts of the expansion coefficients and these hold only for

$$\sqrt{(ka)^2 + (kb)^2} \ll 1.$$

The practical range of validity of these results can be evaluated by comparison with the exact calculations based on Eq.(5) which will be presented later. We will find, for example, that for $b/a = 1$ and $ka = 0.1$ the low frequency approximation for a_0 is in error by less than 1%, for a_2 and a_4 by about 5%, and for a_6 by about 15%. At $ka = 0.25$ the error for a_0 has increased to about 3%, but for a_2 and a_4 it is still about 5%. At $ka = 0.5$ the errors in a_0, a_2 and a_4 are all about 15%. These are only the mathematical errors resulting from approximating Eq.(5) by Eq.(8). The extent to which these results differ from the true solution of the physical problem is another question which we will consider later. It appears that as far as the mathematical errors are concerned the low frequency results in Tables 1-6 are useful for transducer design estimates up to about $ka = 0.25$.

Tables 1-6 in Appendix I show how each expansion coefficient varies with N, that is, with the number of terms used in the expansion. This variation with N reflects how the least squares approximation of the boundary condition changes with the number of terms used. Presumably each change in the approximation is an improvement, and as the approximation settles down the expansion coefficients also settle down to a stable value. The first expansion coefficient stabilizes first, then the second one, etc.. We note that in most cases the first coefficient (a_0 for symmetric problems, a_1 for antisymmetric problems) has stabilized quite well at N = 8 or 9 with some exceptions for b/a far from unity. In many cases the second coefficient also appears to have stabilized well at N = 8 or 9. We will examine the least squares approximations

Fig. 1 The six different cylinders for which low frequency computations were made.

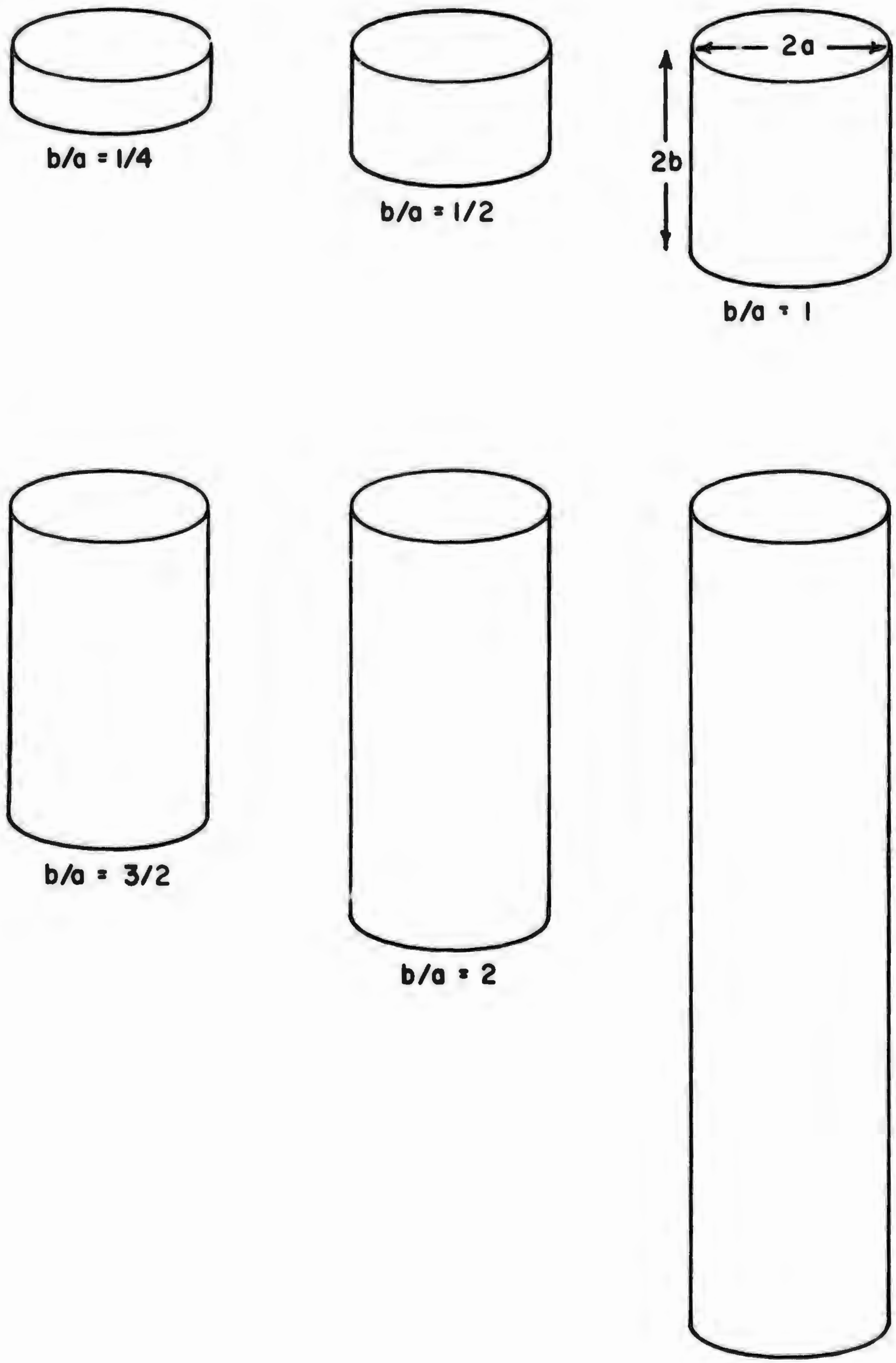

Fig.2 The six different velocity distributions for which low frequency computations were made.

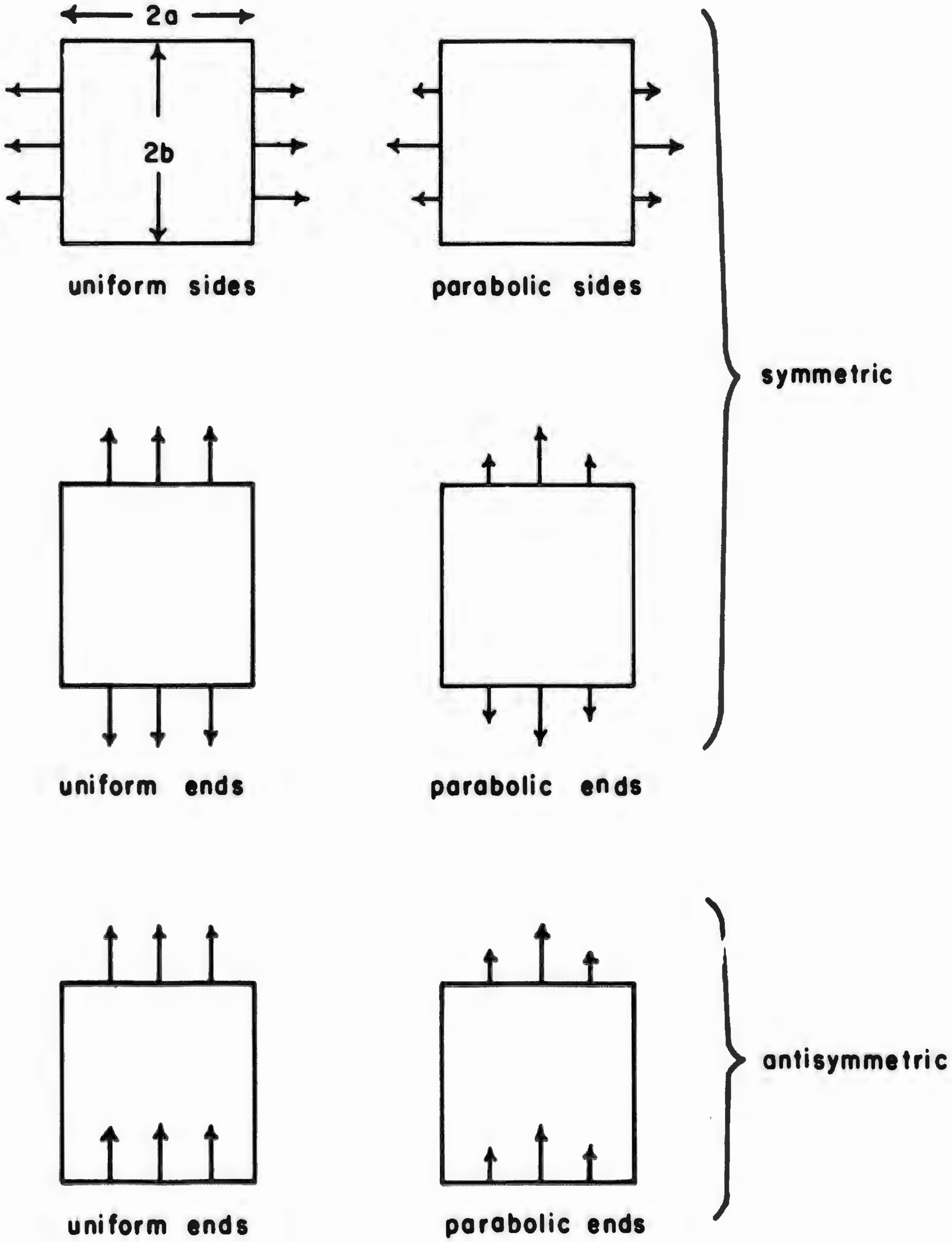

in detail later and try to determine how well these coefficients represent the solutions of the specified problems.

In some cases there is a strong pairing of the expansion coefficients as they vary with N. This can be seen especially for the cases of vibrating ends with $b/a = 1$. We will see later that this behaviour is correlated with the way in which the least squares approximations improve as more terms are added. In certain cases the third term gives little improvement over that obtained with only two terms, and correspondingly the second coefficient does not change appreciably when the third term is added. Then the fifth term gives no improvement over the approximation obtained with four terms, etc. (for example, see Fig 3e).

Evaluation of the Method

Actual Normal Velocity Distributions

From Eq.(1) and the definition of the $\phi_n(\theta)$ we see that the actual normal velocity on the boundary surface is

$$\left.\frac{\partial\psi}{\partial n}\right|_s = \sum_{n=0}^{N} a_n\,\phi_n(\theta). \tag{9}$$

Using Eq.(8) this becomes

$$\left.\frac{\partial\psi}{\partial n}\right|_s = u\sum_{n=0}^{N} b_n\, 1\cdot 1\cdot 3\cdot 5\cdots(2n-1)\begin{cases}\left(\frac{a}{b}\right)^{n+2}(n+1)\cos^{n+2}\theta\, P_{n+1}(\cos\theta)\,, & 0\le\theta\le\theta_0\\[2ex] \sin^{n+3}\theta\, P'_{n+1}(\cos\theta)\,, & \theta_0\le\theta\le\pi/2\end{cases} \tag{10}$$

where b_n is related to a_n by

$$a_n = u(ka)^{n+2}\, b_n / ik. \tag{11}$$

Calculations based on Eq.(10) are shown in some representative cases in Figures 3a - 3f. The specified normal velocity distribution is shown at the top of each figure, and the approximations obtained with one term, two terms, etc. are shown below. These figures show how difficult it is to accurately satisfy boundary conditions on a cylindrical surface by use of spherical wave functions. Figures 3a - 3c show that the approximation is somewhat better for $b/a = 1$ than it is for either large or small b/a. It is evident also that the approximation is better for the parabolic than for the uniform velocity distributions. This is fortunate, because most of the transducer applications are better represented by the parabolic distributions.

The method of calculation determines the expansion coefficients by minimizing the mean square error between the specified and the actual normal velocity for a given number of terms in the expansion. Thus the normal velocity distributions in Figures 3a - 3f are the best fits to the specified distributions in the least squares sense. The root mean square errors between the actual and specified normal velocities were calculated for all the cases treated in the low frequency approximation. These rms errors (E_{rms}) are included in Figures 3a -3f; for example, in Figure 3a for $N = 0$ (one term in the expansion) the rms error is .460 times the magnitude of the velocity of the cylinder sides.

We will not give all the details of the results for the rms errors

Fig. 3a Specified normal velocity $N(\theta)$ and least square approximations $\partial\psi/\partial n\,\big|_s$ (u = 1). Uniform vibration of cylinder sides with b/a = 1.

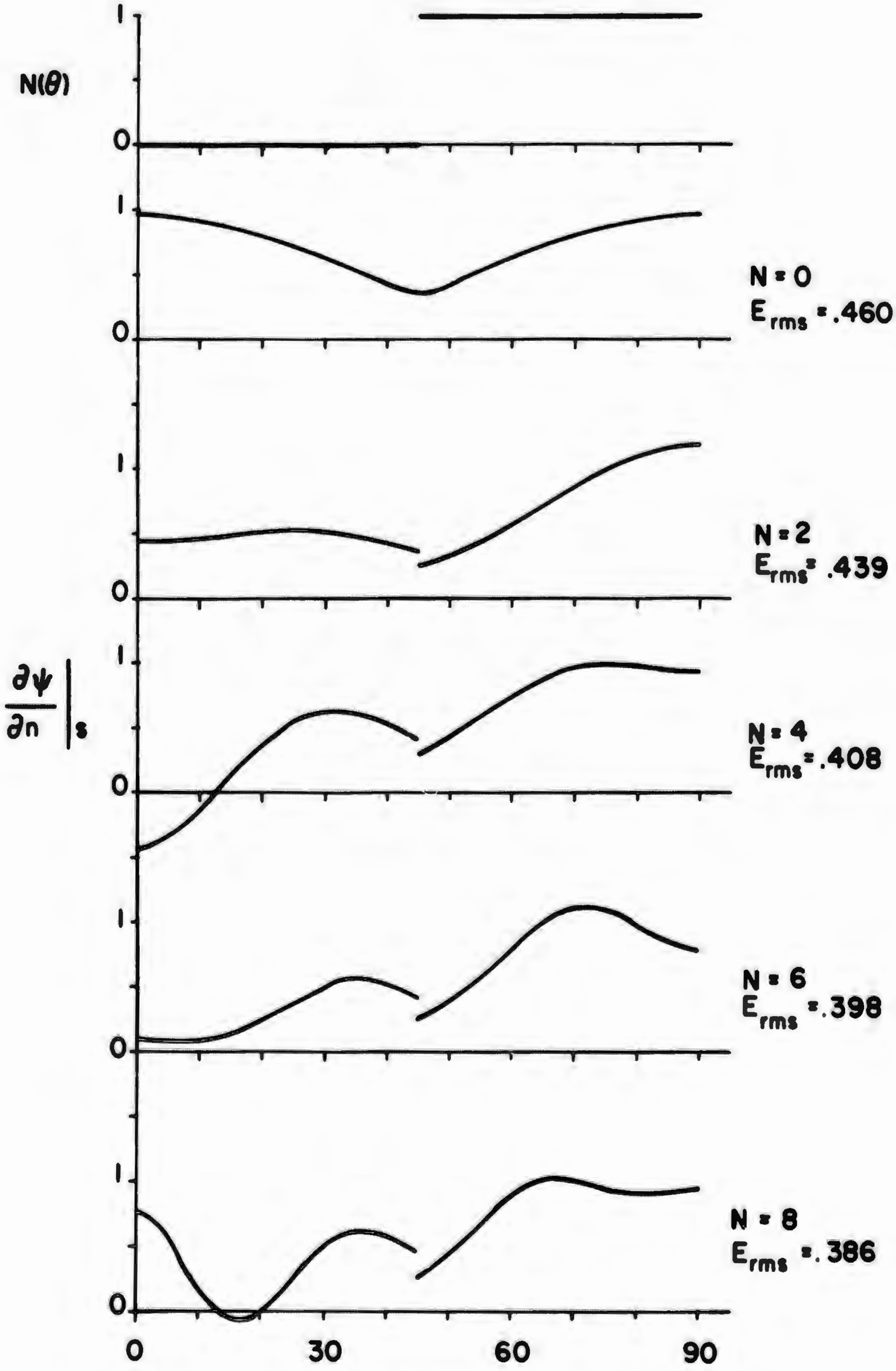

Fig. 3b Uniform vibration of cylinder sides with b/a = 1/4.

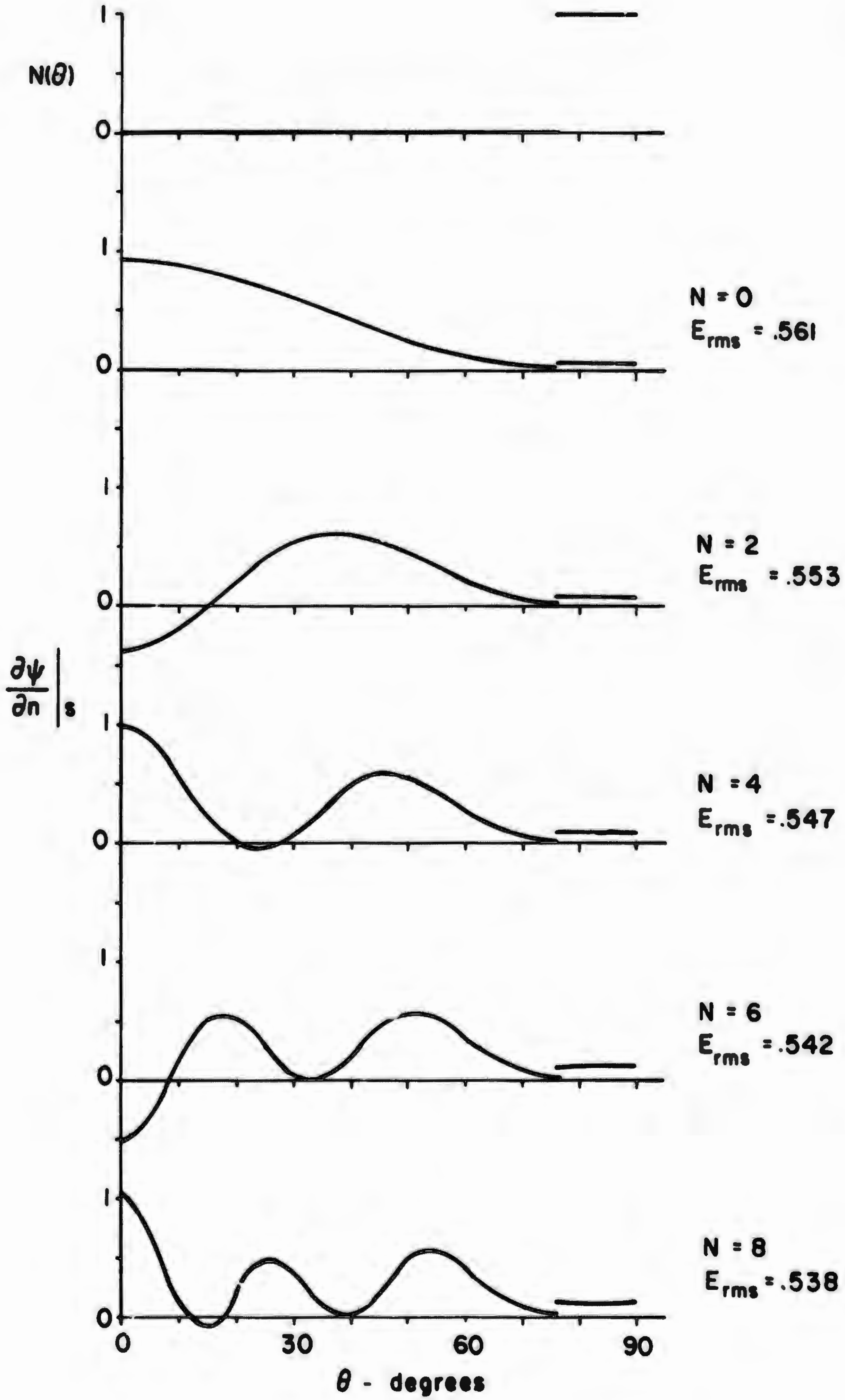

Fig. 3c Uniform vibration of cylinder sides with b/a = 4.

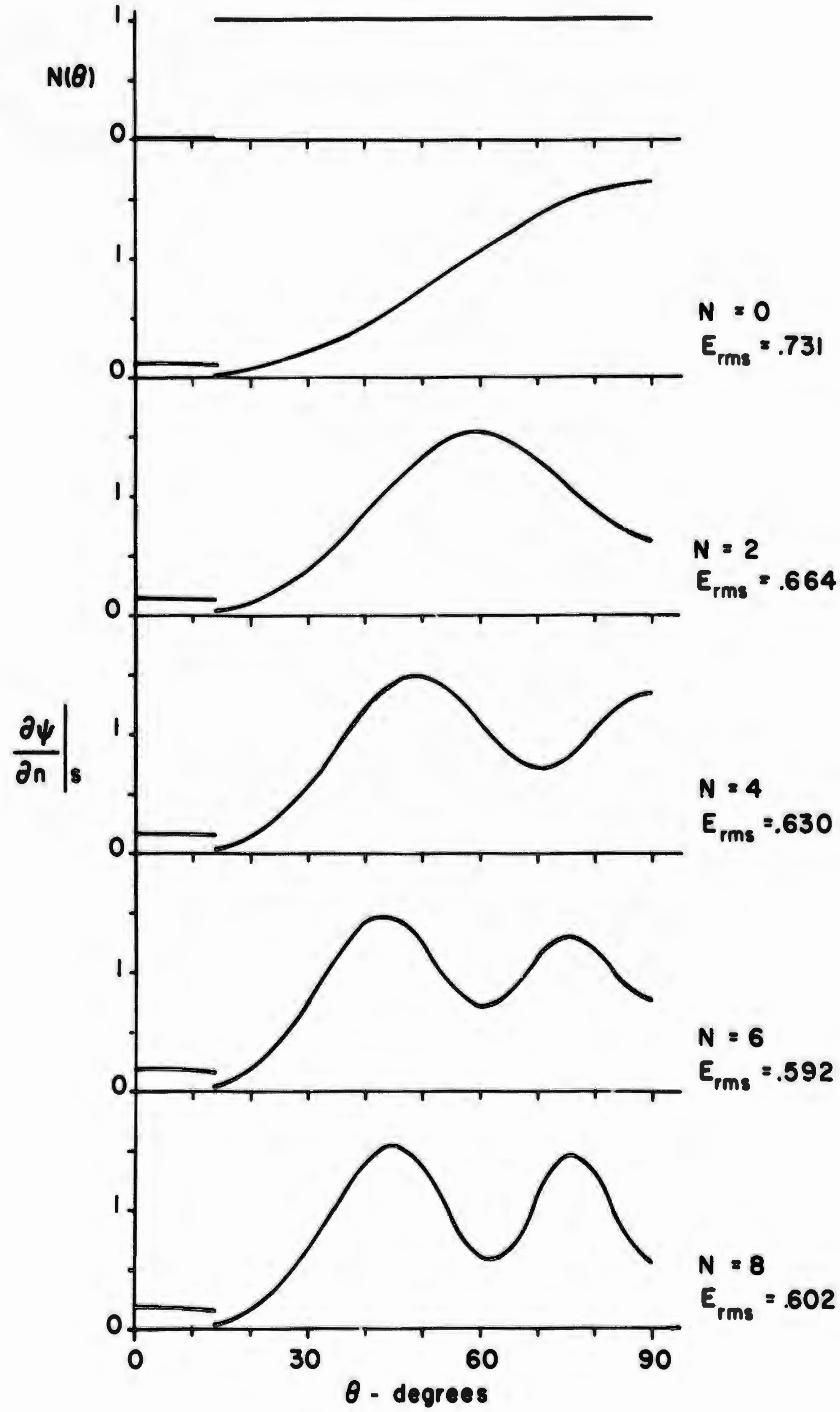

Fig. 3d Parabolic vibration of cylinder sides with b/a = 1.

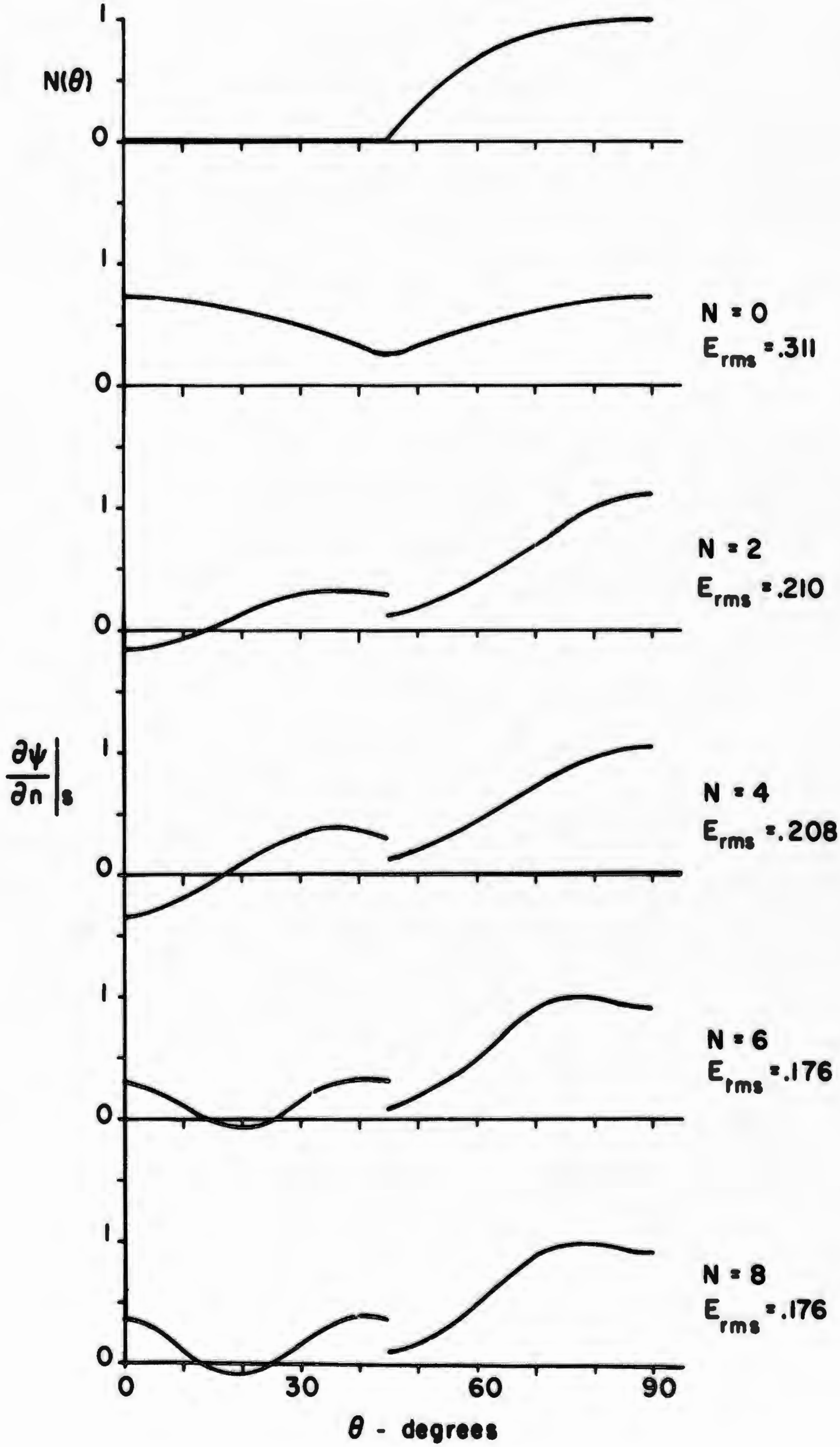

Fig. 3e Uniform vibration of cylinder ends with b/a = 1.

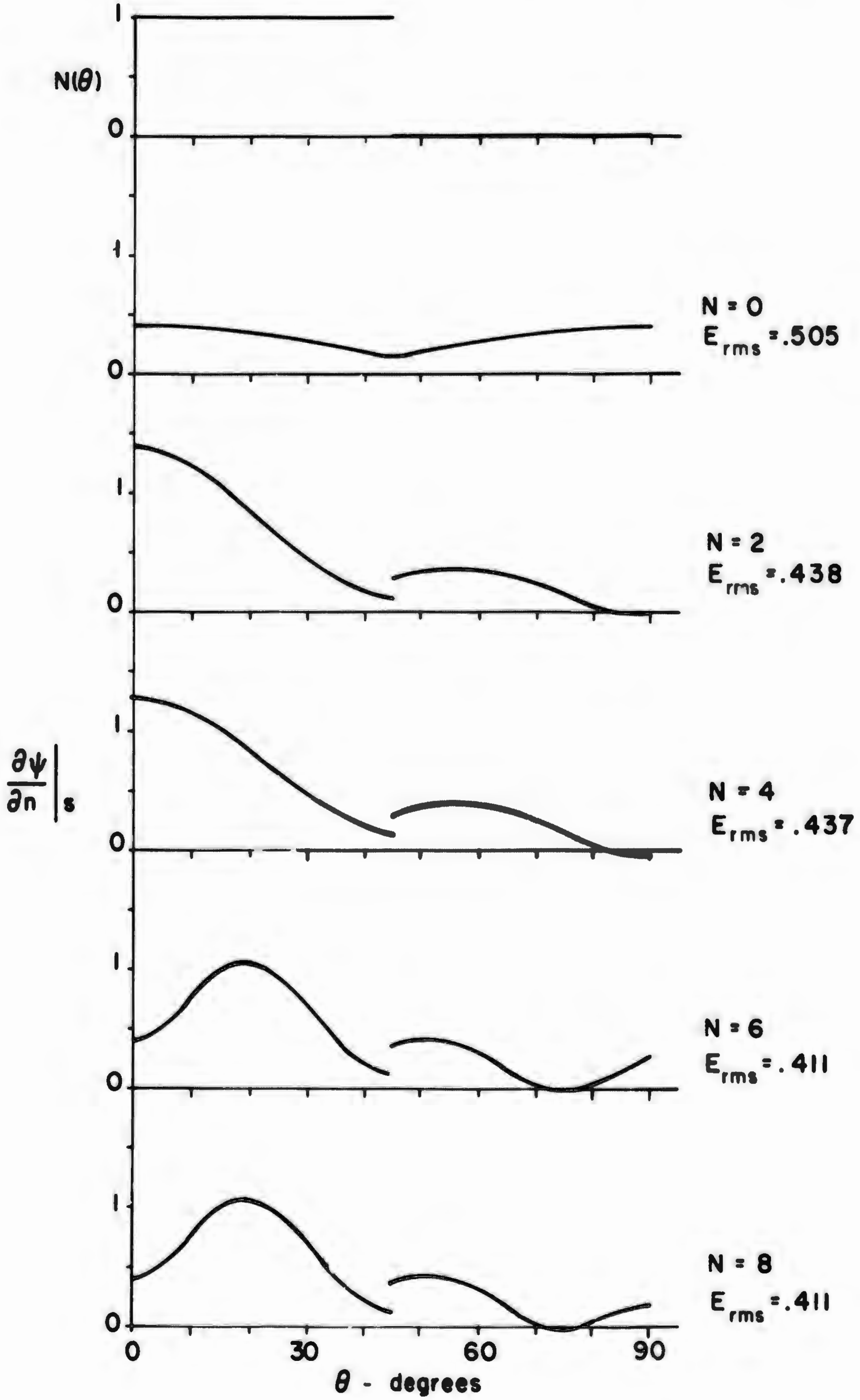

Fig. 3f Parabolic vibration of cylinder ends with b/a = 1.

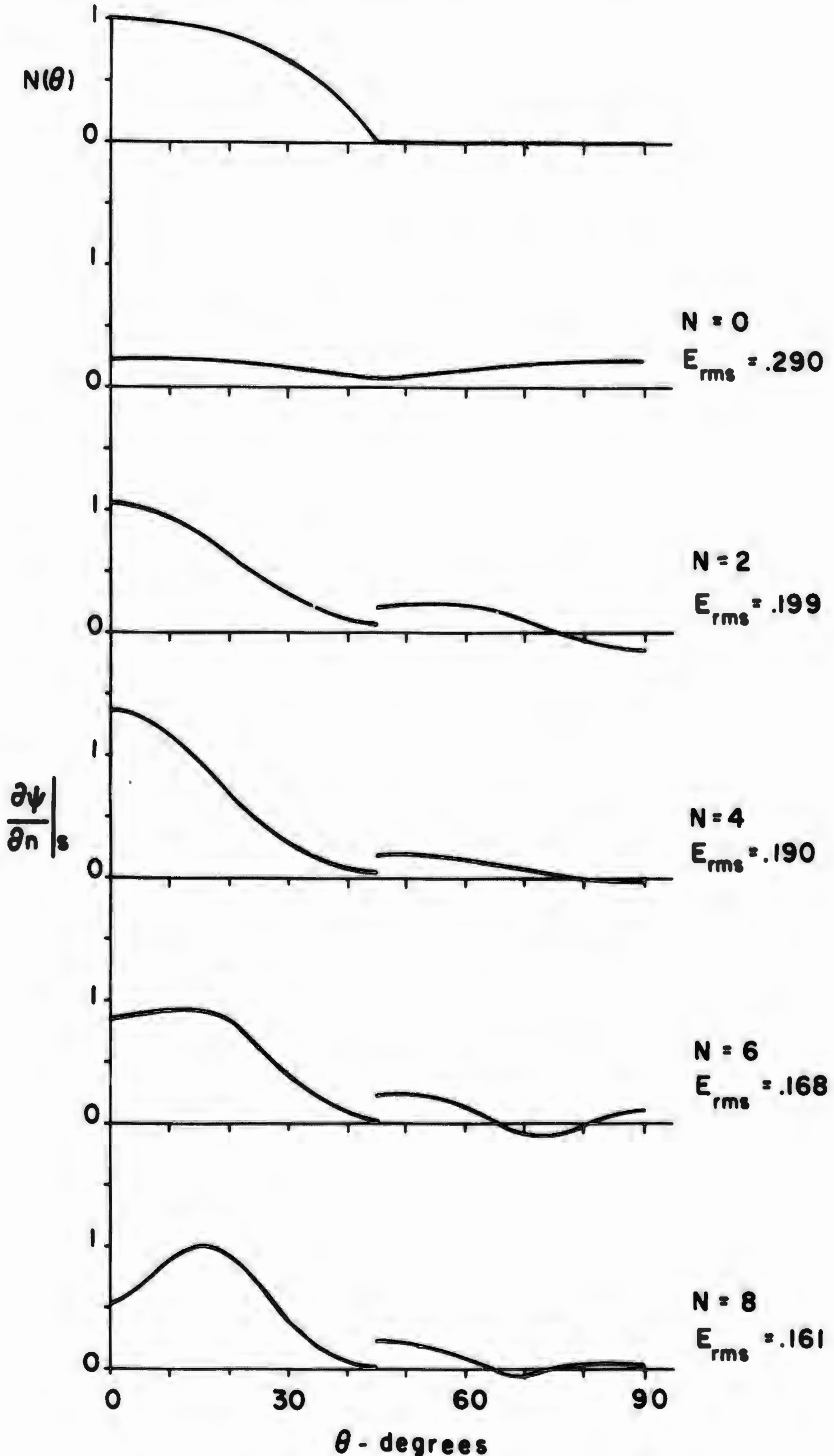

here, since they are not especially illuminating unless they are related carefully to other features of the problem or compared with similar error calculations for other problems. The most significant result found from the error analysis was that in many cases the solutions do not significantly improve as more terms are added; see, for example, Figure 3b. In such cases the method is almost powerless for practical purposes. In other cases the errors decrease quite strongly with the first two or three terms. In general it appears that the results are best for b/a near unity and for parabolic velocity distributions.

Expected Results Based on Radiated Power

For any of the cylinder problems discussed here the radiation resistance can be calculated from the far field using the expression

$$R/\rho c A = \frac{4\pi b^2}{A} \left| \frac{u}{U} \right|^2 \int_0^{\pi/2} \left| \sum_{n=0}^{N} \frac{a_n}{bu} i^{-n} P_n(\cos\theta) \right|^2 \sin\theta \, d\theta \qquad (12)$$

where A is the vibrating area on the cylinder. Eq.(12) gives the radiation resistance referred to U, which is the normal velocity averaged over the vibrating portion of the surface. Thus the time average radiated power is $\frac{1}{2} R|U|^2$.

For sufficiently small ka and kb only the first term of the sum is necessary in the far field. In such cases Eq.(12) gives the results in Table 1, where b_0 and b_1 are the numbers in Appendix I which are related to the expansion coefficients a_0 and a_1 by Eq.(11).

Table 1 Radiation Resistance for the Low Frequency Solutions (The numbers b_0 and b_1 are given in Appendix I)

Symmetric Cases	A	U	$R/\rho c A$
uniform vibration of sides	$4\pi ab$	u	$b_0^2 (ka)^2\, a/b$
parabolic vibration of sides	$4\pi ab$	$2/3\, u$	$9/4\, b_0^2 (ka)^2\, a/b$
uniform vibration of ends	$2\pi a^2$	u	$2 b_0^2 (ka)^2$
parabolic vibration of ends	$2\pi a^2$	$1/2\, u$	$8 b_0^2 (ka)^2$
Antisymmetric Cases			
uniform vibration of ends	$2\pi a^2$	u	$2/3\, b_1^2 (ka)^4$
parabolic vibration of ends	$2\pi a^2$	$1/2\, u$	$8/3\, b_1^2 (ka)^4$

The acoustic power radiated by any sufficiently small pulsating source is equal to that radiated by a monopole sphere of the same source strength. This relationship is most conveniently expressed in the form

$$\frac{1}{A}\left(\frac{R}{\rho c A}\right) = \frac{k^2}{4\pi} \tag{13}$$

where A is the vibrating area of the source in question and R is its radiation resistance referred to its average normal velocity.

This relationship enables us to determine the expected values of b_0 for the symmetric cylinder problems. Using the results in Table 1 we find

$$b_0 = \begin{cases} b/a & \text{uniform vibration of sides} \\ 2/3\, b/a & \text{parabolic vibration of sides} \\ 1/2 & \text{uniform vibration of ends} \\ 1/4 & \text{parabolic vibration of ends.} \end{cases}$$

The values of b_0 for $N = 8$ from Appendix I are compared with these expectations in Table 2.

Table 2 Calculated and Expected Values of the Lowest Order Expansion Coefficient for Low Frequency Symmetric Cases.

	Uniform Sides		Parabolic Sides		Uniform Ends		Parabolic Ends	
b/a	Calculated	Expected	Calculated	Expected	Calculated	Expected	Calculated	Expected
4	2.457	4	2.150	8/3	.089	1/2	.083	1/4
2	1.953	2	1.372	4/3	.426	1/2	.246	1/4
3/2	1.464	3/2	1.026	1	.445	1/2	.263	1/4
1	.993	1	.689	2/3	.463	1/2	.255	1/4
1/2	.507	1/2	.368	1/3	.445	1/2	.248	1/4
1/4	.123	1/4	.083	1/6	.337	1/2	.240	1/4

This comparison shows definite patterns which are consistent with our findings from studying the errors in satisfying the specified boundary conditions. The calculated values of b_0 are close to the expected values for $1/2 \leq b/a \leq 2$, while for $b/a = 4$ or $b/a = 1/4$ the two are quite different in most cases. For vibration of the sides the agreement is better for $b/a = 4$ than $b/a = 1/4$, while for vibrating ends $b/a = 1/4$ gives better agreement. Finally the agreement for the parabolic cases extends to larger b/a for vibrating sides and to smaller b/a for vibrating ends than it does in the uniform cases. The general picture then is that, when using spherical wave functions, the accuracy is best for the cylinder height and diameter approximately equal, but the range of b/a over which a given accuracy could be expected depends on the type of boundary condition.

Exact Calculations

The revised computer program was used to calculate the expansion coefficients for cylinders vibrating symmetrically on the ends. These results are exact in the sense that the exact Eq.(5) was used for the $\phi_n(\theta)$. They still suffer, of course, from the inaccuracies in satisfying the boundary conditions which we have just been discussing. The program includes a modification of the previous boundary conditions in which only a central region on the ends of radius $b \tan\theta_1$ is vibrating, and the outer annular region on the ends is rigid. Calculations have been done for both uniform,

$$N(\theta) = \begin{cases} u, & 0 \leq \theta \leq \theta_1 \\ 0, & \theta_1 \leq \theta \leq \pi/2 , \end{cases}$$

and parabolic,

$$N(\theta) = \begin{cases} u(1 - \tan^2\theta/\tan^2\theta_1) \, . & 0 \leq \theta \leq \theta_1 \\ 0 & , \theta_1 \leq \theta \leq \pi/2 , \end{cases}$$

vibration of the central region on the ends. Results have been obtained for eighteen cases, and the expansion coefficients are given in Appendix II in the form a_n/bu.

The previous remarks about the practical range of validity of the low frequency approximation can now be substantiated by comparison of, for example, Table 3 in Appendix I and the first page of Appendix II for uniform, symmetric vibration of the ends with $b/a = 1$. The agreement at

$ka = 0.1$ can be seen easily, since the factor by which the coefficients differ in these two cases is then a power of ten. Recall that the low frequency approximation gives only the imaginary part of a_n.

Although the revised computer program is more efficient than the original program it still is quite limited in the number of terms which can be handled. However, our study of the least square approximations suggested that simply taking more terms is not always a practical way to improve the solution. The program is useful as it stands, but only for a limited range of b/a near unity and only for far field calculations.

Practical Results

Far Field Patterns

The far field sound pressure can be obtained directly from Eq.(1) and is given by

$$p(r,\theta) = i k \rho c\, \psi(r,\theta) = k b \rho c u \frac{e^{ikr}}{kr} \sum_{n=0}^{N} \frac{a_n}{bu}\, i^{-n} P_n(\cos\theta). \tag{14}$$

The pressure amplitude patterns have been calculated for all the cases where the cylinder dimensions are large enough to give appreciable departures from omnidirectionality.

Figure 4 shows the effect on the pattern of varying the relative amount of vibrating area on the ends for $ka = 1$ and $b/a = 1$. We see the expected minimum in the axial direction where the contributions from the two ends of the cylinder partially cancel. The cancellation is more complete for the smaller sources (smaller θ_1). Since the parabolic velocity distribution corresponds to a smaller effective source it gives a deeper minimum along the axis than the uniform velocity for the same θ_1.

Figures 5 and 6 show patterns for $b/a = 1$ and $\theta_1 = 45^\circ$ (entire ends vibrating) for ka increasing from $1/2$ where the patterns are almost omni-directional to 2 where strong directional effects exist. The directional effects are more pronounced for these sources on the ends of a cylinder than they are for the same sources in a plane, that is, for circular disks of the same ka in a plane.

Figure 7 gives patterns for $ka = 1$, $\theta_1 = \theta_0$ (entire ends vibrating) and $b/a = 0, 1, 2$. The case $b/a = 0$ is, of course, the familiar circular disk in an infinite rigid plane for which the far field is well known for the uniform case (piston) and has been given by Porter[5] for the parabolic case where it is called approximate supported edge case. This reminds us that all the cylinders with height $2b$ and symmetric boundary conditions can equally well be regarded as cylindrical protuberances of height b on an infinite, rigid plane. Similarly the cylinders with antisymmetric boundary conditions can be regarded as protruding from an infinite, ideally soft plane. Fig 7. shows that the maximum on the axis, which occurs for a vibrator in a plane, changes to a minimum (for ka not too large) when the vibrator protrudes from the plane. The deepest minimum for $ka = 1$ probably comes between our two cases of $kb = 1$ and $kb = 2$.

Table 3 gives the pressure amplitude at $\theta = 90^\circ$ relative to the average normal velocity. Specifically the quantity given in the table is

$$P(90^\circ) = \frac{|p(r, 90^\circ)|}{\rho c U} kr = \left| kb \frac{u}{U} \sum_{n=0}^{N} \frac{a_n}{bu} i^{-n} P_n(0) \right| \qquad (15)$$

Fig. 4 Normalized far field pressure amplitude. symmetric vibration of ends

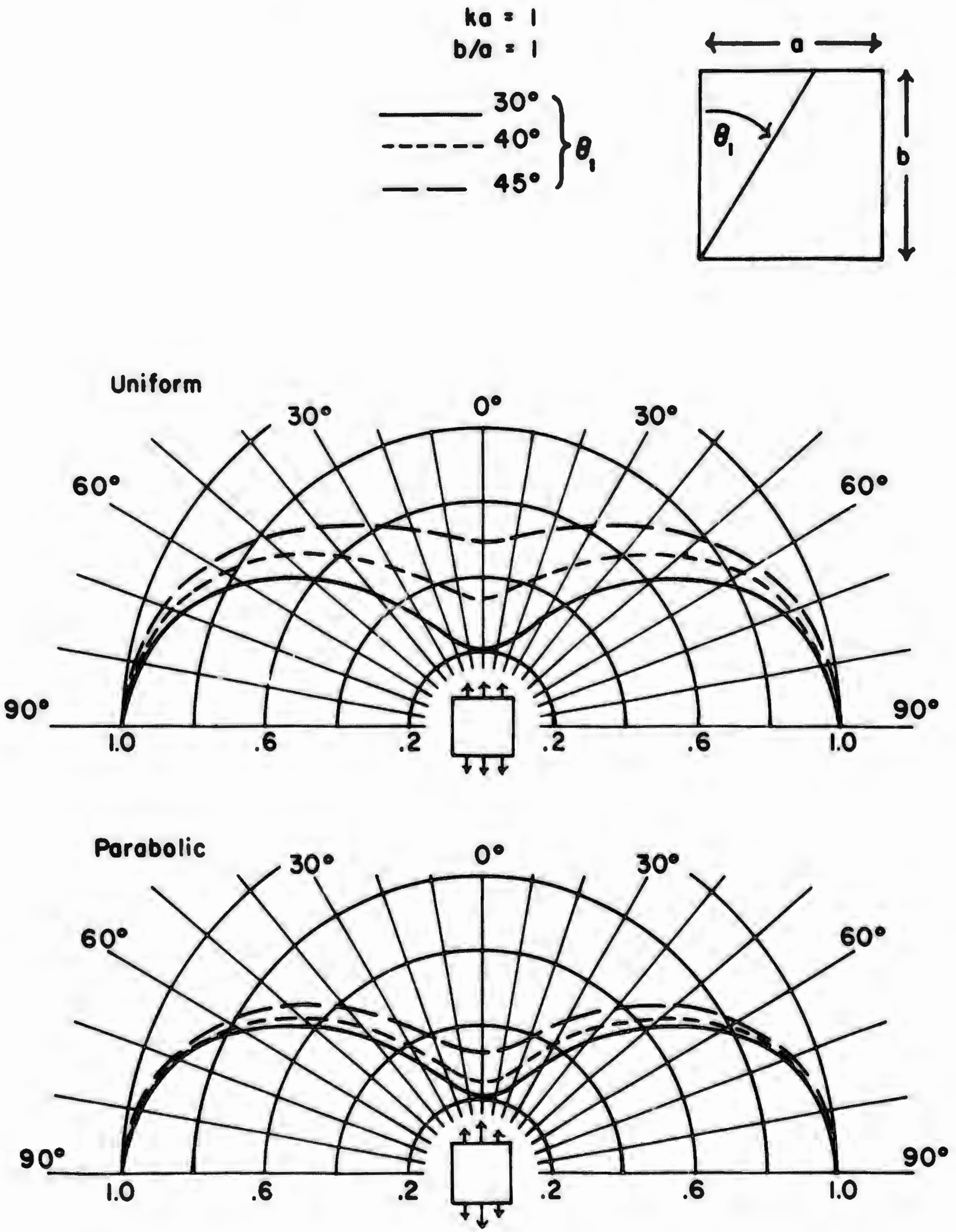

Fig. 5 Normalized far field pressure amplitude
Uniform symmetric vibration of entire ends
b/a = 1

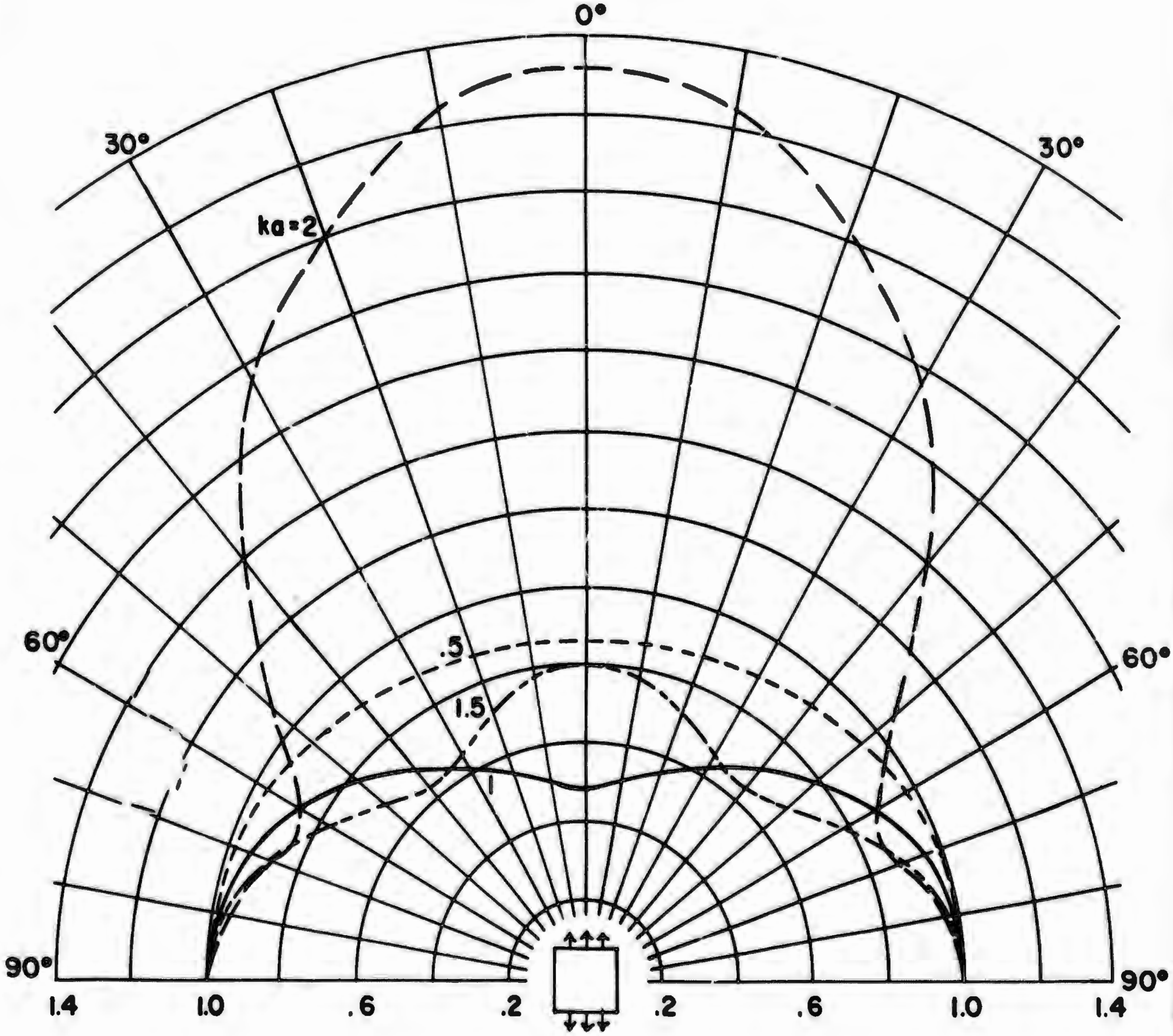

Fig. 6 Normalized far field pressure amplitude
Parabolic symmetric vibration of entire ends
b/a = 1

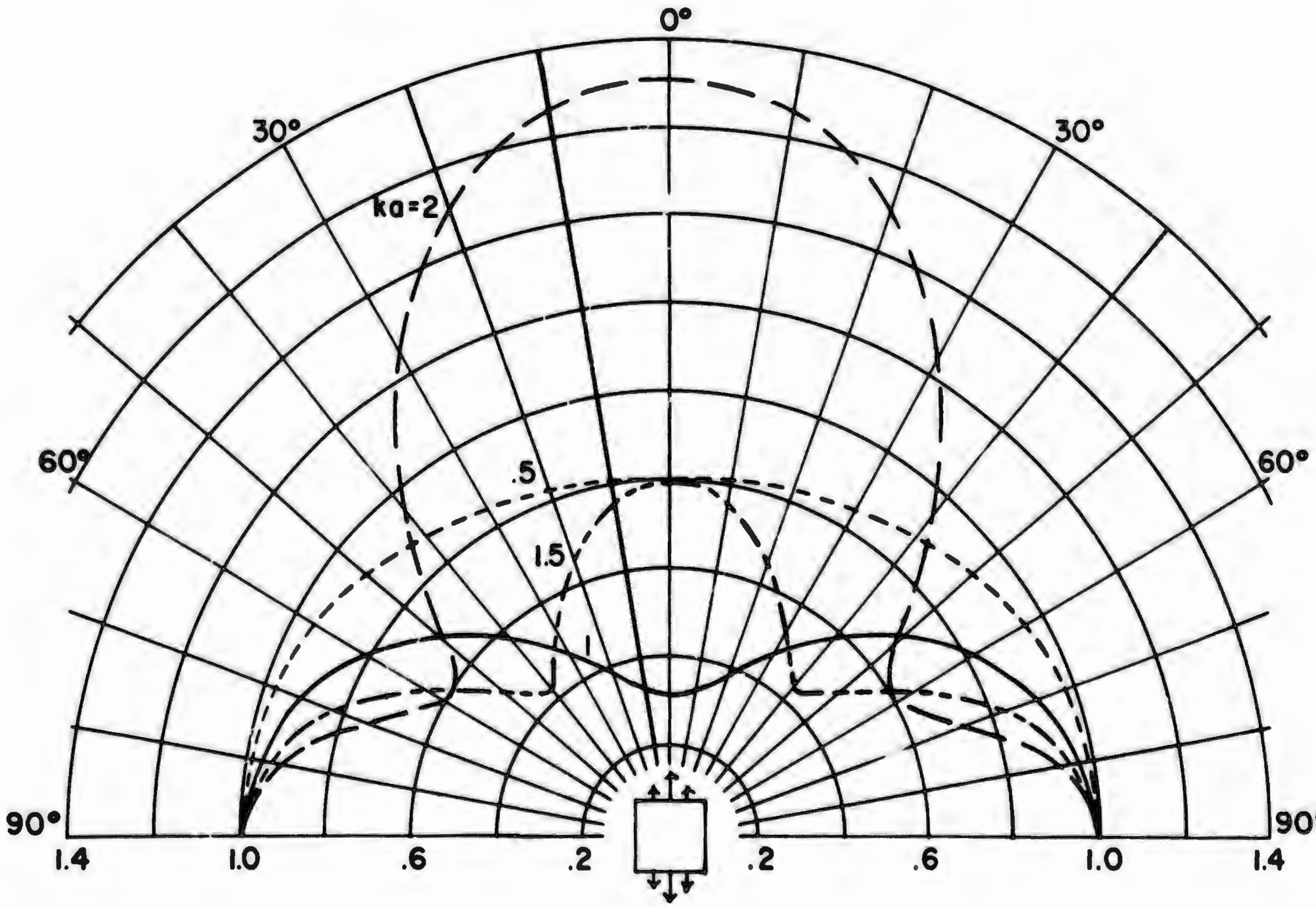

Fig. 7 Normalized far field pressure amplitude
symmetric vibration of ends

ka = 1

—— b/a = 0

— — b/a = 1

- - - - b/a = 2

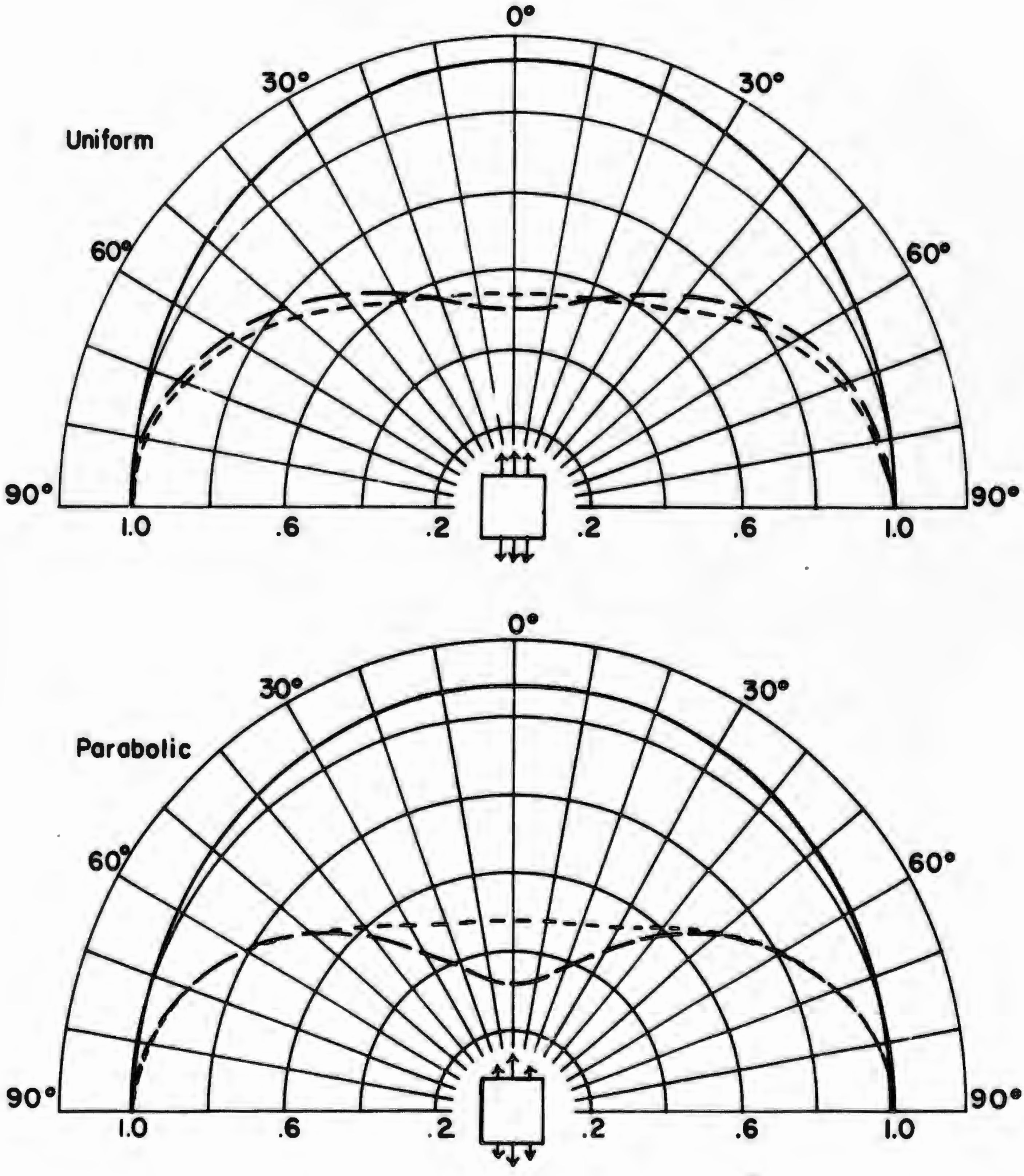

where U is the average normal velocity; $U = u$ for uniform vibration, while $U = \frac{1}{2} u$ for parabolic vibration. With the results in Table 3 the normalized patterns in Figs. 4 - 7 can be compared on an absolute basis.

Table 3. Pressure amplitude at 90° (see Eq.(15)) and radiation resistance for cylinders vibrating on the ends (referred to average normal velocity).

			Uniform		Parabolic	
ka	b/a	θ_1	$P(90°)$	$R/\rho cA$	$P(90°)$	$R/\rho cA$
1	1	30°	.161	.087	.159	.084
1	1	40°	.306	.169	.330	.181
1	1	θ_0	.369	.194	.434	.234
.5	1	θ_0	.108	.085	.119	.099
1	1	θ_0	.369	.194	.434	.234
1.5	1	θ_0	.699	.292	.955	.444
2	1	θ_0	.778	.470	1.272	.747
1	0	θ_0	.440	.423	.460	.42
1	1	θ_0	.369	.194	.434	.234
1	2	θ_0	.248	.084	.278	.099

These far field calculations require only three or four terms in the expansion for the largest ka and kb which have been used. Reasonably stable values of these first few coefficients have been obtained by taking terms up to $N = 16$ in the machine calculations. In Appendix II the coefficients are given only for the maximum value of N used and that value of N is indicated.

Radiation Resistance

For the cylinders vibrating on the ends where $A = 2\pi b^2 \tan^2 \theta_1$, we have for the radiation resistance

$$R/\rho c A = \frac{2}{\tan^2\theta_1} \left|\frac{u}{U}\right|^2 \int_0^{\pi/2} \left| \sum_{n=0}^{N} \frac{a_n}{bu}\, i^{-n} P_n(\cos\theta) \right|^2 \sin\theta \, d\theta . \tag{16}$$

The results calculated from Eq.(16) by numerical integration of the far field patterns are given in Table 3. Figure 8 also shows $R/\rho c A$ as a function of ka for $b/a = 1$ with the disk in a plane case $(b/a = 0)$ for comparison. The curve for $b/a = 0$ and parabolic vibration is from reference 5. The important point for practical applications shown by these results is the significant decrease of the radiation resistance when the vibrator protrudes from the plane of symmetry. This is also shown clearly in Table 3 for the cases with $ka = 1$ and $b/a = 0, 1$ and 2.

Conclusion

The work described here has been aimed mainly at discovering the practical limitations of the previously proposed method of calculating acoustic radiation from a cylinder. It appears that when using spherical wave functions useful far field information, such as directivity patterns and radiation resistance, can be obtained for cylinders with height to diameter ratio between about 2 and 1/2. New information of this kind has

Fig. 8 Radiation resistance referred to average velocity for vibrating circular disks of radius a on the ends of a rigid cylinder of height 2b.

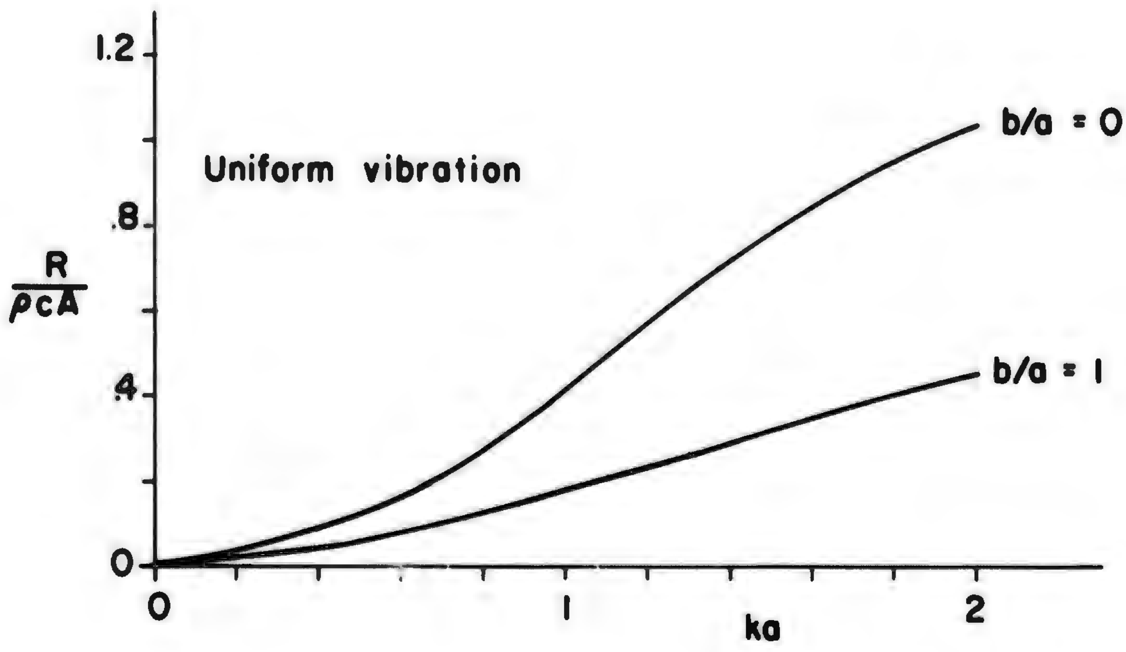

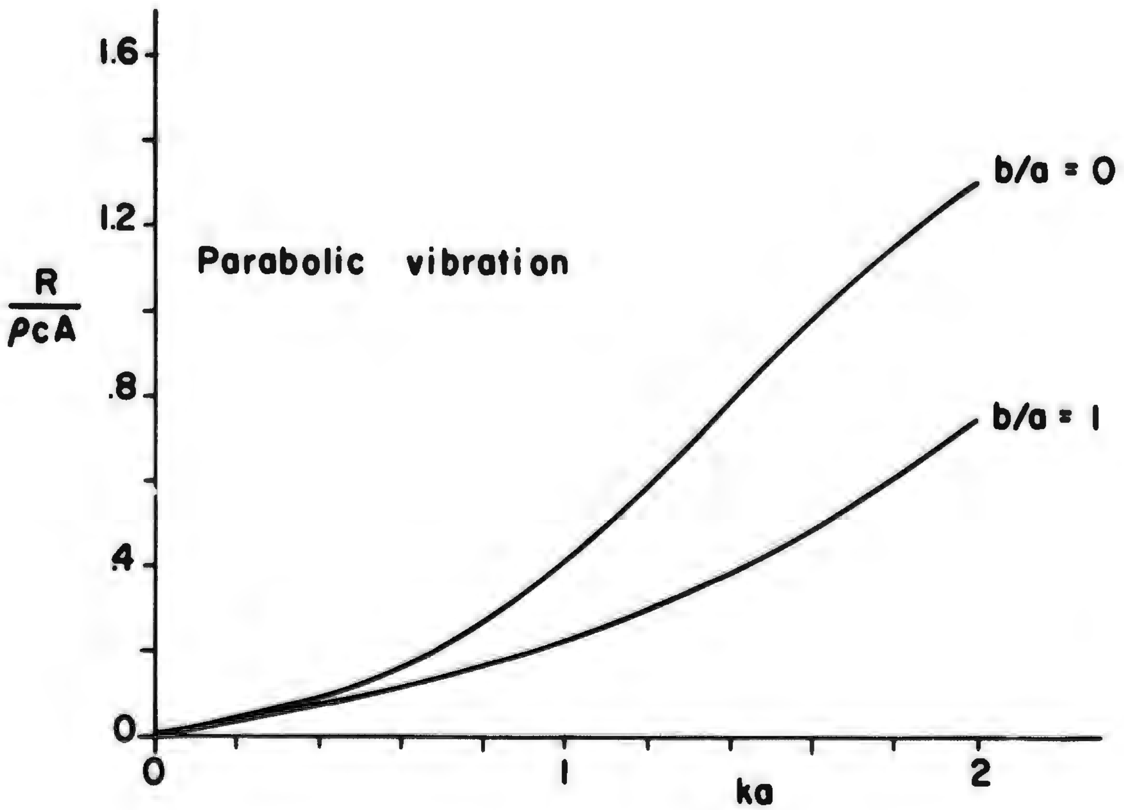

been given here, and additional calculations could be made with the existing computer program. However, it has not been possible to use enough terms to get reliable near field information.

We have also seen that the range of usefulness of the method depends in a quite detailed way on the boundary conditions. For example, when using spherical wave functions for a cylinder, it depends on whether the sides or the ends of the cylinder are vibrating and on the shape of the velocity distribution. These findings support the obvious need for investigating the use of other wave functions, and suggest that a fruitful direction for future work would be the development of wave functions which could be adjusted to suit specific boundary shapes and specific boundary values.

Acknowledgement

The writers are grateful to Wentworth Williams and N. G. Parke for continuing discussions and to Benjamin T. Howard and Nan E. Gordon for assistance with computations and drawings.

References

1) W. Williams, N. G. Parke, D. A. Moran and C. H. Sherman, J. Acoust. Soc. Am. 36 2316-2322 (1964).

2) PML Staff, "Acoustic Radiation from a Finite Cylinder - Numerical Results", PML Scientific Report No. 1, Contract N140(70024)75686B, June 1964.

3) C. H. Sherman, "Acouctic Radiation from a Finite Cylinder - Low Frequency Approximation", PML Tech. Memo. No. 2, Contract N140(70024)-75686B, May 1965.

4) P. M. Morse and H. Feshback, Methods of Theoretical Physics, McGraw Hill Book Co., New York, 1953, p. 1575.

5) D. T. Porter, J. Acoust. Soc. Am. 36 1154-1161 (1964).

Appendix I

Expansion Coefficients Calculated in the Low Frequency Approximation

In the low frequency approximation only the imaginary parts of the expansion coefficients are given, and the approximation is valid for $\sqrt{(ka)^2+(kb)^2} << 1$. The results are obtained as functions of ka when b/a is numerically specified. Thus we have tabulated the quantities $ika_n/u(ka)^{n+2}$. The notation .1642E1, for example, means .1642 x 10'.

Table 1 Uniform, symmetric vibration of cylinder sides.

Table 2 Parabolic, symmetric vibration of cylinder sides.

Table 3 Uniform, symmetric vibration of cylinaer ends.

Table 4 Parabolic, symmetric vibration of cylinder ends.

Table 5 Uniform, antisymmetric vibration of cylinder ends.

Table 6 Parabolic, antisymmetric vibration of cylinder ends.

BLANK PAGE

Table 1 Uniform Symmetric Vibration of Sides

N	$ika_0 / u(ka)^2$	$ika_2 / u(ka)^4$	$ika_4 / u(ka)^6$	$ika_6 / u(ka)^8$	$ika_8 / u(ka)^{10}$
			$b/a = 4$		
0	.1642 E1				
2	.2083 E1	.3143 E0			
4	.2335 E1	.6082 E0	.8900 E-2		
6	.2511 E1	.8727 E0	.2317 E-1	.1048 E-3	
8	.2457 E1	.7757 E0	.1603 E-1	.8213 E-5	-.2755 E-6
			$b/a = 2$		
0	.1472 E1				
2	.1776 E1	.2304 E0			
4	.1895 E1	.3869 E0	.4889 E-2		
6	.1942 E1	.4718 E0	.7733 E-2	.3656 E-4	
8	.1953 E1	.5002 E0	.1202 E-1	.6898 E-4	.9503 E-7
			$b/a = 3/2$		
0	.1310 E1				
2	.1453 E1	.1244 E0			
4	.1450 E1	.1176 E0	-.2378 E-3		
6	.1445 E1	.6652 E-1	-.4165 E-2	-.3418 E-4	
8	.1464 E1	.4870 E-1	-.7980 E-2	-.1080 E-3	-.2575 E-6

Table 1 Uniform Symmetric Vibration of Sides

N	$ika_0 / u(ka)^2$	$ika_2 / u(ka)^4$	$ika_4 / u(ka)^6$	$ika_6 / u(ka)^8$	$ika_8 / u(ka)^{10}$
			$b/a = 1$		
0	.9660 E 0				
2	.9422 E 0	-.5628 E-1			
4	.9858 E 0	-.6020 E-1	-.1665 E-2		
6	.9778 E 0	-.7878 E-1	-.1688 E-2	.9646 E-5	
8	.9932 E 0	-.8061 E-1	-.2331 E-2	.9980 E-5	.5523 E-7
			$b/a = 1/2$		
0	.3279 E 0				
2	.4293 E 0	-.1729 E-1			
4	.4768 E 0	-.3410 E-1	.1277 E-3		
6	.4988 E 0	-.4815 E-1	.3276 E-3	-.3722 E-6	
8	.5066 E 0	-.5874 E-1	.6461 E-3	-.1142 E-5	.5600 E-9
			$b/a = 1/4$		
0	.5745 E-1				
2	.8253 E-1	-.7396 E-3			
4	.9981 E-1	-.1562 E-2	.1394 E-5		
6	.1121 E 0	-.2384 E-2	.3884 E-5	-.1083 E-8	
8	.1226 E 0	-.3185 E-2	.7205 E-5	-.3743 E-8	.4589 E-12

Table 2 Parabolic Symmetric Vibration of Sides

N	$ika_0/u(ka)^2$	$ika_2/u(ka)^4$	$ika_4/u(ka)^6$	$ika_6/u(ka)^8$	$ika_8/u(ka)^{10}$
			$b/a = 4$		
0	.1523E1				
2	.1880 E1	.2548 E0			
4	.2067 E1	.4716 E0	.6566 E-2		
6	.2187 E1	.6524 E0	.1632 E-1	.7162 E-4	
8	.2150 E1	.5858 E0	.1142 E-1	.5364 E-5	-.1890 E-6
			$b/a = 2$		
0	.1246 E1				
2	.1384 E1	.1044 E0			
4	.1401 E1	.1275 E0	.7194 E-3		
6	.1389 E1	.1058 E0	-.5175 E-3	-.9334 E-5	
8	.1372 E1	.6468 E-1	-.3831 E-2	-.5623 E-4	-.1375 E-6
			$b/a = 3/2$		
0	.1056 E1				
2	.1057 E1	.8139 E-3			
4	.1023 E1	-.6635 E-1	-.2360 E-2		
6	.1019 E1	-.1111 E0	-.5795 E-2	-.2993 E-4	
8	.1026 E1	-.1180 E0	-.7246 E-2	-.5840 E-4	-.9926 E-7

Table 2 Parabolic Symmetric Vibration of Sides

N	$ika_0/u(ka)^2$	$ika_2/u(ka)^4$	$ika_4/u(ka)^6$	$ika_6/u(ka)^8$	$ika_8/u(ka)^{10}$
			$b/a = 1$		
0	.7279 E0				
2	.6880 E0	-.9460E-1			
4	.6971 E0	-.9542E-1	-.3468 E-3		
6	.6874 E0	-.1180 E0	-.3143 E-3	.1171 E-4	
8	.6888 E0	-.1181 E0	-.3768 E-3	.1174 E-4	.4977 E-8
			$b/a = 1/2$		
0	.2282 E0				
2	.3034 E0	-.1282 E-1			
4	.3412 E0	-.2622 E-1	.1019 E-3		
6	.3604 E0	-.3846 E-1	.2759 E-3	-.3241 E-6	
8	.3680 E0	-.4872 E-1	.4876 E-3	-.1070 E-5	.5427 E-9
			$b/a = 1/4$		
0	.3876 E-1				
2	.5578 E-1	-.5017 E-3			
4	.6720 E-1	-.1062 E-2	.9498 E-6		
6	.7596 E-1	-.1624 E-2	.2652 E-5	-.7402 E-9	
8	.8313 E-1	-.2174 E-2	.4930 E-5	-.2566 E-8	.3149 E-12

Table 3 Uniform Symmetric Vibration of Ends

N	$ika_0/u(ka)^2$	$ika_2/u(ka)^4$	$ika_4/u(ka)^6$	$ika_6/u(ka)^8$	$ika_8/u(ka)^{10}$
			$b/a = 4$		
0	.5055 E-1				
2	.6920 E-1	.1331 E-1			
4	.8224 E-1	.2849 E-1	.4594 E-3		
6	.9278 E-1	.4432 E-1	.1314 E-2	.6276 E-5	
8	.8954 E-1	.3856 E-1	.8896 E-3	.5361 E-6	-.1637 E-7
			$b/a = 2$		
0	.1737 Eo				
2	.2633 Eo	.6792 E-1			
4	.3324 Eo	.1583 Eo	.2825 E-2		
6	.3865 Eo	.2571 Eo	.8462 E-2	.4255 E-4	
8	.4260 Eo	.3528 Eo	.1617 E-1	.1517 E-3	.3198 E-6
			$b/a = 3/2$		
0	.2645 Eo				
2	.3945 Eo	.1130 Eo			
4	.4438 Eo	.2095 Eo	.3377 E-2		
6	.4474 Eo	.2490 Eo	.6420 E-2	.2645 E-4	
8	.4453 Eo	.2509 Eo	.6826 E-2	.3441 E-4	.2774 E-7

PARKE MATHEMATICAL LABORATORIES, INCORPORATED
ONE RIVER ROAD • CARLISLE, MASSACHUSETTS

Table 3 Uniform Symmetric Vibration of Ends

N	$ika_0/u(ka)^2$	$ika_2/u(ka)^4$	$ika_4/u(ka)^6$	$ika_6/u(ka)^8$	$ika_8/u(ka)^{10}$
			$b/a = 1$		
0	.4001 E0				
2	.4440 E0	.1040 E0			
4	.4494 E0	.1035 E0	−.2068 E−3		
6	.4625 E0	.1340 E0	−.2508 E−3	−.1583 E−4	
8	.4628 E0	.1340 E0	−.2661 E−3	−.1582 E−4	.1219 E−8
			$b/a = 1/2$		
0	.4058 E0				
2	.4560 E0	−.8641 E−2			
4	.4575 E0	−.9192 E−2	.4191 E−5		
6	.4503 E0	−.4566 E−2	−.6162 E−4	.1225 E−6	
8	.4452 E0	.2348 E−2	−.2042 E−3	.6250 E−6	−.3654 E−9
			$b/a = 1/4$		
0	.1794 E0				
2	.2469 E0	−.1989 E−2			
4	.2874 E0	−.3975 E−2	.3368 E−5		
6	.3157 E0	−.5792 E−2	.8878 E−5	−.2394 E−8	
8	.3371 E0	−.7432 E−2	.1566 E−4	−.7835 E−8	.9886 E−12

Table 4 Parabolic Symmetric Vibration of Ends

N	$ika_0/u(ka)^2$	$ika_2/u(ka)^4$	$ika_4/u(ka)^6$	$ika_6/u(ka)^8$	$ika_8/u(ka)^{10}$
			b/a = 4		
0	.5045 E-1				
2	.6673 E-1	.1162 E-1			
4	.7734 E-1	.2397 E-1	.3740 E-3		
6	.8554 E-1	.3629 E-1	.1039 E-2	.4881 E-5	
8	.8302 E-1	.3180 E-1	.7019 E-3	.4071 E-6	-.1276 E-7
			b/a = 2		
0	.9111 E-1				
2	.1425 E0	.3852 E-1			
4	.1842 E0	.9303 E-1	.1703 E-2		
6	.2189 E0	.1564 E0	.5317 E-2	.2727 E-4	
8	.2459 E0	.2218 E0	.1059 E-1	.1019 E-3	.2189 E-6
			b/a = 3/2		
0	.1444 E0				
2	.2263 E0	.7118 E-1			
4	.2698 E0	.1564 E0	.2981 E-2		
6	.2747 E0	.2109 E0	.7172 E-2	.3642 E-4	
8	.2629 E0	.2221 E0	.9553 E-2	.8313 E-4	.1628 E-6

Table 4 Parabolic Symmetric Vibration of Ends

N	$ika_0/u(ka)^2$	$ika_2/u(ka)^4$	$ika_4/u(ka)^6$	$ika_6/u(ka)^8$	$ika_8/u(ka)^{10}$
			$b/a = 1$		
0	.2344 E0				
2	.2711 E0	.8703 E-1			
4	.2547 E0	.8850 E-1	.6254 E-3		
6	.2624 E0	.1065 E0	.5994 E-3	-.9347 E-5	
8	.2552 E0	.1074 E0	.9266 E-3	-.9505 E-5	-.2607 E-7
			$b/a = 1/2$		
0	.2801 E0				
2	.2800 E0	.1283 E-4			
4	.2687 E0	.5774 E-2	-.4378 E-4		
6	.2524 E0	.1298 E-1	-.1463 E-3	.1909 E-6	
8	.2477 E0	.1942 E-1	-.2793 E-3	.6596 E-6	-.3409 E-9
			$b/a = 1/4$		
0	.1444 E0				
2	.1903 E0	-.1353 E-2			
4	.2145 E0	-.2540 E-2	.2013 E-5		
6	.2296 E0	-.3509 E-2	.4949 E-5	-.1277 E-8	
8	.2399 E0	-.4296 E-2	.9208 E-5	-.3888 E-8	.4504 E-12

Table 5 Uniform Antisymmetric Vibration of Ends

N	$ika_1/u(ka)^3$	$ika_3/u(ka)^5$	$ika_5/u(ka)^7$	$ika_7/u(ka)^9$	$ika_9/u(ka)^{11}$
$b/a = 4$					
1	.2592 E-1				
3	.4953 E-1	.2169 E-2			
5	.7166 E-1	.5676 E-2	.4778 E-4		
7	.9265 E-1	.1013 E-1	.1580 E-3	.4848 E-6	
9	.1161 E0	.1615 E-1	.3643 E-3	.2176 E-5	.3307 E-8
$b/a = 2$					
1	.1584 E0				
3	.3256 E0	.1578 E-1			
5	.4876 E0	.4307 E-1	.3817 E-3		
7	.6332 E0	.7734 E-1	.1271 E-2	.4016 E-5	
9	.7696 E0	.1189 E-0	.2810 E-2	.1719 E-4	.2647 E-7
$b/a = 3/2$					
1	.2849 E0				
3	.5372 E0	.2649 E-1			
5	.6699 E0	.5686 E-1	.4829 E-3		
7	.6893 E0	.7088 E-1	.9818 E-3	.2649 E-5	
9	.6865 E0	.7135 E-1	.1032 E-2	.3252 E-5	.1466 E-8

Table 5 Uniform Antisymmetric Vibration of Ends

N	$ika_1/u(ka)^3$	$ika_3/u(ka)^5$	$ika_5/u(ka)^7$	$ika_7/u(ka)^9$	$ika_9/u(ka)^{11}$
			$b/a = 1$		
1	.4256 E0				
3	.4478 E0	.1051 E-1			
5	.5125 E0	.1033 E-1	-.1518 E-3		
7	.5234 E0	.1476 E-1	-.1570 E-3	-.8218 E-6	
9	.5509 E0	.1470 E-1	-.2372 E-3	-.8132 E-6	.2975 E-8
			$b/a = 1/2$		
1	.1166 E0				
3	.2114 E0	-.1972 E-2			
5	.2764 E0	-.4450 E-2	.8294 E-5		
7	.3135 E0	-.6522 E-2	.2142 E-4	-.1461 E-7	
9	.3292 E0	-.7764 E-2	.3297 E-4	-.3928 E-7	.1285 E-10
			$b/a = 1/4$		
1	.9524 E-2				
3	.1842 E-1	-.4443 E-4			
5	.2656 E-1	-.1148 E-3	.5623 E-7		
7	.3407 E-1	-.2017 E-3	.1822 E-6	-.3336 E-10	
9	.4102 E-1	-.2991 E-3	.3775 E-6	-.1294 E-9	.1142 E-13

Table 6 Parabolic Antisymmetric Vibration of Ends

N	$ika_1/u(ka)^3$	$ika_3/u(ka)^5$	$ika_5/u(ka)^7$	$ika_7/u(ka)^9$	$ika_9/u(ka)^{11}$
$b/a = 4$					
1	.1330 E-1				
3	.2844 E-1	.1385 E-2			
5	.4435 E-1	.3907 E-2	.3436 E-4		
7	.6071 E-1	.7373 E-2	.1202 E-3	.3776 E-6	
9	.8004 E-1	.1235 E-1	.2907 E-3	.1775 E-5	.2732 E-8
$b/a = 2$					
1	.8828 E-1				
3	.2202 E0	.1245 E-1			
5	.3662 E0	.3704 E-1	.2440 E-3		
7	.5060 E0	.6996 E-1	.1198 E-2	.3857 E-5	
9	.6410 E0	.1111 E0	.2720 E-2	.1689 E-4	.2619 E-7
$b/a = 3/2$					
1	.1698 E0				
3	.3758 E0	.2164 E-1			
5	.4921 E0	.4824 E-1	.4231 E-3		
7	.5078 E0	.5951 E-1	.8252 E-3	.2136 E-5	
9	.5118 E0	.5877 E-1	.7548 E-3	.1284 E-5	-.2070 E-8

Table 6 Parabolic Antisymmetric Vibration of Ends

N	$ika_1/u(ka)^3$	$ika_3/u(ka)^5$	$ika_5/u(ka)^7$	$ika_7/u(ka)^9$	$ika_9/u(ka)^{11}$
			$b/a = 1$		
1	.2921 E0				
3	.3070 E0	.7062 E-2			
5	.3827 E0	.6851 E-2	-.1776 E-3		
7	.3927 E0	.1092 E-1	-.1824 E-3	-.7535 E-6	
9	.4292 E0	.1083 E-1	-.2888 E-3	-.7421 E-6	.3949 E-8
			$b/a = 1/2$		
1	.1114 E0				
3	.2256 E0	-.2375 E-2			
5	.3159 E0	-.5814 E-2	.1151 E-4		
7	.3736 E0	-.9050 E-2	.3201 E-4	-.2282 E-7	
9	.4020 E0	-.1129 E-1	.5281 E-4	-.6724 E-7	.2223 E-10
			$b/a = 1/4$		
1	.1234 E-1				
3	.2463 E-1	-.6137 E-4			
5	.2637 E-1	-.1629 E-3	.8113 E-7		
7	.4756 E-1	-.2924 E-3	.2690 E-6	-.4973 E-10	
9	.5820 E-1	-.4415 E-3	.5678 E-6	-.1969 E-9	.1749 E-13

Appendix II

Expansion Coefficients Obtained From the Computer Program

The quantities tabulated here are a_n/b_u , and all results are for cylinders vibrating symmetrically on the ends. The notation -2.401E-5, for example, means -2.401×10^{-5}.

Eighteen different cases, including uniform and parabolic velocity distributions, are given in the following order:

ka	b/a	θ_1	N
.1	1	45°	8
.25	1	45°	10
.5	1	45°	12
1	1	45°	16
1.5	1	45°	16
2	1	45°	16
1	1	30°	14
1	1	40°	14
1	2	θ_0	14

The value of N given is the maximum value used, and the expansion coefficients are given only for this value of N

BLANK PAGE

$ka = .1$	$b/a = 1$	$\theta_1 = 45°$ $N = 8$
n	Uniform	Parabolic
0	−2.401 E−5 − i 4.630 E−2	−1.171 E−5 − i 2.549 E−2
2	−9.213 E−9 − i 1.420 E−4	−4.495 E−9 − i 1.130 E−4
4	4.285 E−12 + i 2.564 E−9	2.091 E−12 − i 9.338 E−9
6	1.107 E−16 + i 1.820 E−12	5.399 E−17 + i 1.132 E−12
8	−9.293 E−21 − i 6.163 E−19	−4.535 E−21 + i 2.654 E−17
$ka = .25$	$b/a = 1$	$\theta_1 = 45°$ $N = 10$
0	−8.734 E−4 − i 1.143 E−1	−4.266 E−4 − i 6.274 E−2
2	−2.249 E−6 − i 2.544 E−3	−1.098 E−6 − i 1.940 E−3
4	6.145 E−9 + i 2.571 E−7	3.004 E−9 − i 9.079 E−7
6	1.578 E−12 + i 1.902 E−9	7.688 E−13 + i 1.114 E−9
8	−5.232 E−16 − i 4.638 E−15	−2.559 E−16 + i 1.001 E−13
10	−4.652 E−20 − i 5.700 E−17	−2.265 E−20 − i 3.045 E−17

$ka = .5$	$b/a = 1$	$\theta_1 = 45°$ $N = 12$
n	Uniform	Parabolic
0	−1.112 E−2 − i 2.056 E−1	−5.457 E−3 − i 1.107 E−1
2	−7.874 E−5 − i 1.968 E−2	−3.859 E−5 − i 1.527 E−2
4	1.482 E−6 + i 5.667 E−6	7.306 E−7 − i 8.618 E−5
6	8.938 E−10 + i 2.382 E−7	4.322 E−10 + i 1.422 E−7
8	8.145 E−12 + i 6.487 E−12	−1.553 E−12 + i 9.872 E−11
10	−4.199 E−16 − i 1.147 E−13	−2.019 E−16 − i 6.261 E−14
12	5.739 E−19 − i 2.887 E−18	2.837 E−19 − i 1.954 E−1[illegible]

$ka = 1$	$b/a = 1$	$\theta_1 = 45°$ $N = 16$
0	−7.004 E−2 − i 6.943 E−2	−3.536 E−2 − i 3.935 E−2
2	−2.857 E−3 − i 6.276 E−2	−1.603 E−3 − i 3.909 E−2
4	9.383 E−5 − i 1.791 E−3	4.309 E−5 − i 1.152 E−3
6	2.987 E−7 − i 3.018 E−6	1.439 E−7 − i 1.869 E−6
8	−4.677 E−9 + i 3.835 E−8	−2.243 E−9 + i 2.705 E−8
10	−1.433 E−11 + i 7.845 E−11	−7.147 E−12 + i 5.850 E−11
12	1.773 E−15 − i 8.487 E−16	9.128 E−16 − i 1.921 E−15
14	2.749 E−17 − i 1.679 E−18	1.420 E−17 − i 2.280 E−17
16	1.506 E−20 + i 3.083 E−20	7.889 E−21 + i 6.362 E−21

$ka = 1.5$	$b/a = 1$	$\theta_1 = 45°$ $N = 16$
n	Uniform	Parabolic
0	− 2.189 E−1 − i 2.591 E−1	−1.142 E−1 − i 1.412 E−1
2	1.447 E−1 − i 3.672 E−1	7.133 E−2 − i 3.281 E−1
4	4.833 E−3 − i 1.241 E−4	2.639 E−3 − i 9.992 E−3
6	− 1.640 E−4 + i 4.928 E−4	− 8.376 E−5 + i 3.194 E−4
8	−1.195 E−6 + i 4.504 E−7	−6.603 E−7 + i 2.747 E−6
10	1.011 E−8 − i 3.183 E−8	5.254 E−9 − i 1.855 E−8
12	3.132 E−11 − i 1.707 E−11	1.740 E−11 − i 7.368 E−11
14	− 7.202 E−14 + i 2.312 E−13	− 3.775 E−14 + i 1.284 E−13
16	−1.172 E−16 + i 7.476 E−17	− 6.531 E−17 + i 2.777 E−16

$ka = 2$	$b/a = 1$	$\theta_1 = 45°$ $N = 16$
0	− 3.343 E−1 − i 1.276 E−1	−1.801 E−1 − i 7.827 E−2
2	5.160 E−1 − i 6.175 E−1	2.574 E−1 − i 4.578 E−1
4	3.343 E−2 + i 5.602 E−3	1.896 E−2 − i 3.452 E−2
6	− 1.806 E−3 + i 2.289 E−3	−9.559 E−4 + i 1.233 E−3
8	− 2.727 E−5 − i 1.301 E−6	−1.567 E−5 + i 3.026 E−5
10	3.566 E−7 − i 4.821 E−7	1.928 E−7 − i 2.165 E−7
12	2.300 E−9 − i 3.925 E−11	1.330 E−9 − i 2.581 E−9
14	− 8.134 E−12 + i 1.127 E−11	−4.443 E−12 + i 4.664 E−12
16	− 2.748 E−14 + i 1.504 E−15	−1.593 E−14 + i 3.089 E−14

$ka=1$	$b/a=1$	$\theta_1=30°$ $N=14$
n	Uniform	Parabolic
0	− 3.118 E−2 −i 1.069 E−1	−1.566 E−2 −i 5.265 E−2
2	1.567 E−3 −i 1.008 E−1	8.317 E−4 −i 5.011 E−2
4	8.257 E−6 −i 2.253 E−3	4.159 E−5 −i 1.404 E−3
6	−3.558 E−7 +i 7.264 E−6	−1.875 E−7 −i 3.098 E−6
8	− 3.001 E−9 +i 1.041 E−7	−1.512 E−9 +i 2.931 E−8
10	4.554 E−12 +i 3.308 E−11	2.390 E−12 +i 5.453 E−11
12	9.031 E−15 −i 3.114 E−13	4.551 E−15 −i 4.943 E−14
14	−6.525 E−18 −i 1.462 E−16	−3.418 E−18 −i 6.617 E−17
$ka=1$	$b/a=1$	$\theta_1=40°$ $N=14$
0	− 6.465 E−2 −i 2.264 E−1	−3.267 E−2 −i 1.144 E−1
2	3.298 E−3 −i 1.451 E−1	1.652 E−3 −i 9.350 E−2
4	1.672 E−4 −i 8.663 E−4	8.577 E−5 −i 1.534 E−3
6	−6.940 E−7 +i 3.221 E−6	−3.659 E−7 +i 1.101 E−5
8	−6.025 E−9 +i 5.377 E−8	−3.107 E−9 +i 6.119 E−8
10	8.643 E−12 −i 4.019 E−10	4.637 E−12 −i 1.022 E−10
12	1.806 E−14 −i 1.964 E−13	9.337 E−15 −i 1.858 E−13
14	−1.223 E−17 +i 5.665 E−16	−6.613 E−18 +i 1.232 E−16

$ka = 1$	$b/a = 2$	$\theta_1 = 0^\circ$ $N = 14$
n	Uniform	Parabolic
0	− 9.041 E−2 −i 2.923 E−1	− 4.588 E−2 −i 1.578 E−1
2	4.829 E−3 −i 1.320 E−1	2.363 E−3 −i 1.072 E−1
4	2.299 E−4 +i 8.320 E−5	1.190 E−4 −i 1.183 E−3
6	− 9.477 E−7 +i 3.026 E−5	− 6.006 E−7 +i 1.719 E−5
8	− 8.229 E−9 +i 4.895 E−9	− 4.293 E−9 +i 5.104 E−8
10	1.150 E−11 −i 3.870 E−10	6.247 E−12 −i 1.921 E−10
12	2.459 E−14 −i 2.557 E−14	1.287 E−14 −i 1.610 E−13
14	− 1.607 E−17 +i 5.556 E−16	− 8.847 E−18 +i 2.586 E−16